Proceedings of Ninth World Conference on Earthquake Engineering
August 2-9, 1988, Tokyo-Kyoto, JAPAN (Vol.IV)

6-2-11

A STUDY ON MAXIMUM LOAD CARRYING CAPACITY OF H-SHAPED STEEL BEAM-TO-COLUMN CONNECTIONS

Yoshiro MUKUDAI[1], Akira MATSUO[1] and Shuichi TANAKA[2]

[1]Department of Structural Engineering, Hiroshima University, Saijo-Cho, Higashi-Hiroshima, Japan

[2]Nagoya Special Building Sales Office, Sekisui House, Ltd, Nakamura-ku, Nagoya, Japan

SUMMARY

Eight experimental specimens including X and T-type steel subassemblages were selected to apply numerical analyses in order to make the resisting mechanism of the beam-to-column connections clear. It was found that the increase in strength of a beam-to-column connection after yielding of a panel plate is equivalent to the sum of the local moment transmitted directly between the beams and columns through the intersections of their flanges, and that the ultimate bending moment and large moment gradient along the flanges and stiffeners is achieved near the intersections. On the basis of these numerical results, a predicting method of the maximum strength of a connection is suggested in this paper.

INTRODUCTION

Many tests have been conducted to investigate the plastic behavior of steel beam-to-column connections, which are reviewed by B.Kato(Ref.1). Most of these researches are carried out on the basis of the design philosophy that the beam-to-column connections should be strong enough for us to expect the beams and columns to achieve the full plastic moment and to absorb most of any earthquake energy. This has become the standard idea in designing the steel structures in Japan.

M.Nakao(Ref.2) suggested that the beam-to-column subassemblages whose connections are designed weaker than the beams and columns have enough energy absorption capacity for us to be able to make much of it for aseismatic design of steel structures. A.Kawano et al.(Ref.4) proposed the ultimate aseismatic design method of panel-collapsed type steel structures where the restriction about the width-to-thickness ratio of the flanges and webs and the interval of the lateral supports can be loosened. We believe that these design methods where we expect a connection to absorb the earthquake energy are profitable for the design of low or middle-rise buildings whose columns tend to yield much earlier than beams. In order to realize them it is necessary to evaluate the maximum load carrying capacity of the connection to protect the beams and columns from entirely yielding. D.J.Fielding et al.(Ref.5), E.P.Popov et al.(Ref.6) and M.Nakao(Ref.3) have suggested a predicting method of the shear force(panel moment)-shear deformation relation of a connection after the yielding of a panel plate. But these proposed methods do not always give us a good approximation to the experimental results, because they are not based on the real resisting mechanism of the beam-to-column connections. We have also conducted many experimental and analytical studies in order to make it clear. In this paper we selected eight specimens and compared these experimental results with the FEM numerical results and suggested a resist-

ing mechanism and an evaluating method of the maximum strength of the connections.

EXPERIMENTAL METHOD AND SPECIMENS

We prepared the X-type and T-type specimens. The X-type specimen is illustrated in Fig.1 and the details of all the specimens are indicated in Tab.1 and 2. The first letter of the name indicates the shape of the specimen. Anti-symmetrical loadings were given to the tops of the beam in a monotonously increasing manner after a constant axial thrust(0.0 or $0.3N_y$, N_y:yielding thrust) was given to the column. α and R_{py} in Tab.1 are defined as follows.

$$\alpha = {}_pM_y / \Sigma_m M_p \quad (1)$$

$$R_{py} = P_{py} / P_{my} \quad (2)$$

where ${}_pM_y$ is the yield panel moment(=$(H_c - c t_f)(H_b - b t_f) c t_w \tau_y$, $H_c, c t_f, c t_w$: column height, flange and web thickness, $H_b, b t_f$: beam height and flange thickness and τ_y :yielding shear stress), $\Sigma_m M_p$ is the sum of the plastic moments of the weaker members joining to the connection, Ppy is the yielding load of the panel plate and P_{my} is the yielding load of the weaker member between the beam and column. We selected various combinations of beams and columns whose α ranges from 0.2 to 0.6 in order to obtain the various types of panel moment(pM)- shear deformation(γ) relations. The measuring frame for the shear deformation of the panel, the displacement transducers(DG) and the wire strain gages(WSG) are illustrated in Fig.1.

ANALYTICAL METHOD

We adopted the constant strain triangular element(Ref.8) of a plain stress condition and the beam element(Ref.7). An analytical model of the subassemblages is illustrated in Fig.2. A subassemblage is divided into two areas -- a connection area and the other area --. In the connection area the beam element of a rectangular section is used for idealizing the flanges and horizontal stiffeners and the constant strain triangular element is used for the beam and column webs. The beam element of an H-shaped section is used for idealizing the beams and columns outside of the connection area. These two areas are connected according to the condition that the plane remains plain after deformation. An example of mesh division is illustrated in Fig.3. The beam elements nearest to the intersection of the beam and column flanges are supposed to be always elastic considering the reinforcement of the bead of the fillet weld. The stress-strain relation is assumed to be bilinear with the strain hardening modulus (E_{st}) of E/100 for the beam elements and E/200 for the triangular elements. In the triangular element, von Mises' yield criterion is adopted and the stress-strain incremental stiffness matrix is introduced according to Y.Yamada(Ref.8). Lastly the geometrical nonlinearity is neglected in the analyses.

EXPERIMENTAL AND ANALYTICAL RESULTS

The panel moment(pM) - shear deformation(γ) relations obtained in the experiments are illustrated in Fig.4. We have obtained various types of ${}_pM - \gamma$ relations. We selected eight specimens to make analyses, which are numbered in Fig.4 and correspond to the specimens (1)TMB0-3-0850A, (2)TMB0-4-1050, (3)TMB0-3-1250, (4)TMB0-4-1250A, (5)XMC0-4-0920, (6)XMC3-4-0920B, (7)XMC3-2-1130, (8)XMC3-2-1140. Three of the numerically obtained ${}_pM - \gamma$ relations of the connections are illustrated in Figs.5 compared with the experimental results. The resisting moment against the PΔ effect is included in the panel moment. The numerical results indicated by 'total' approximate well to the experimental results. The dotted line indicated by 'panel' shows the panel moment shared by the panel plate itself, which is calculated from the average shearing stress of the triangular elements in the panel. The differences between these two curves show the rein-

forcement by neighboring beams and columns. The moment distributions along the flanges and horizontal stiffners at the stage when the plastic modulus of 'total' is almost the same as that of 'panel' are illustrated in Figs.6. These figures show that the total moment of the horizontal stiffner and the column flange of the column side are balanced with that of the beam flange and the column flange of the beam side at the intersection point of the beam and column flanges. The total of these total moments of one side for four corners of a connection is illustrated by ●⟶○ in Figs.5 and it is clear that this corresponds to the difference between 'total' and 'panel' which is equivalent to the reinforcement by the beams and columns adjacent to the connection.

Table 3 shows the bending moment of the flanges or stiffeners at the boundary between the unyielding and usual flange elements. M_{fp} and M_{fu} is the full plastic moment and ultimate bending strength of the flanges and stiffeners. They are defined by the following expressions.

$$M_{fp} = Z_f\sigma_y\{1-(N_f/A_f\sigma_y)^2\} \quad (3)$$

$$M_{fu} = Z_f\sigma_B\{1-(N_f/A_f\sigma_B)^2\} \quad (4)$$

where Z_f, A_f is the plastic section modulus and the area of a flange or a stiffner, σ_B is the tensile strength, N_f is the axial force at ${}_pM={}_pM_y$. This table shows that most of the bending moments of the flanges and stiffners exceeded the full plastic moment at an early stage($\gamma/\gamma_y=8\sim17$), and they have arrived at the ultimate strength at the end of the analysis($\gamma/\gamma_y=20\sim40$). It is very interesting that the moment gradient near the intersection of the beam and column flanges is very large in Figs.6. This area corresponds to the plastic regions in the beam and column which are illustrated in Fig.7. The small plastic area near the intersection in a beam and a column also suggests the direct transmission of local moments between them. Fig.8 indicates the moment gradient(shear forces) along the unyielding element at the final step of the analyses. Q_{fy} is the yielding shear force of the flange and stiffner. They are much scattered, ranging from 0.2 to $0.45Q_{fy}$ and $0.32Q_{fy}$ is obtained as the averaged shear force. This shear force along the unyielding element includes the resisting effects of the web against the local moment. As the amount of this shear force may depend upon the existence of scallop and combination of a flange and a web, we need much more research to know it. Fig.9 illustrates an example of the axial force distributions along the flanges and stiffners at the same loading step as Fig.6(b). This figure shows that axial force along the flanges and stiffners surrounding the panel is less than half of that along the beam and column flanges.

THE ULTIMATE STRENGTH OF BEAM-TO-COLUMN CONNECTIONS

The ultimate strength($_pM_u$) of the beam-to-column connections are evaluated by the following method on the basis of the discussions made above.

$$_pM_u = {}_pM_{u1} + \Sigma {}_pM_{u2} \quad (5)$$

where Σ indicates the total about the four corners of the panel. $_pM_{u1}$ is the ultimate shear strength of a panel plate. It is assumed that the shearing stress in the panel reaches the ultimate shear strength($\tau_u=\sigma_B/\sqrt{3}$) of the steel without shear buckling. Then,

$$_pM_{u1} = \tau_u t_p(H_b-{}_bt_f)(H_c-{}_ct_f) \quad (6)$$

is obtained, where t_p is the panel thickness. $_pM_{u2}$ is the ultimate reinforcement by the beams and columns adjacent to the panel. We assume that the reinforcement after the yielding of the panel is achieved by the direct transmission of loacal bending moments between the beam and the column through the intersections of the flanges. The ultimate strength of this local moment is given in the following way.

$$_pM_{u2} = \min\{\Sigma_b(M_{fu}+Q_fL_r),\ \Sigma_c(M_{fu}+Q_fL_r)\} \quad (7)$$

$$M_{fu} = Z_f\sigma_B\{1-(N/A_f\sigma_B)^2\} \quad (8)$$

where Σ_b indicates the total of the beam flange and the column flange at the beam side and Σ_c indicates the total of the horizontal stiffner and the column flange at the column side. N is the axial force along the beam and column flanges at ${}_pM = {}_pM_{ul}$, and half of N is taken for the axial force along the column flanges and stiffners surrounding the panel plate. L_r is the measured length between the intersection point and the toe of the fillet weld. Q_f is the shear force along the unyielding element. As it depends much upon the details of the welded joint and combination of the flange and the web, it is temporarily supposed to be $0.3Q_{fy}$ on the basis of the numerical results(Fig.8). The moment distribution along the outer column flange adjacent to the connection of the T-type subassemblages is assumed to be linear(Fig.6(b)). The ultimate strength of the specimens listed in Table 1 is obtained according to this method and is compared with the experimental results in Table4. In this table L_r is given in terms of the thickness, and the superscript c,e indicates the computed and experimental results. This table shows that the predicted strength approximates well to the experimental results.

CONCLUSIONS

We applied the numerical analyses to the eight specimens and obtained the following conclusions by comparing them with the experimental results.

1)The increase in strength of a beam-to-column connection after yielding of a panel plate is equivalent to the local moment transmitted directly between the beams and columns through the intersections of their flanges.

2)The ultimate bending strength M_{fu} of the flanges and stiffners is achieved near this intersection.

3)The moment gradient along the unyielding element near this intersection is very large and $0.32Q_{fy}$ is obtained as an averaged value.

4)We suggested a predicting method of the maximum strength of beam-to-column connections, which gives a good approximation to the experimental results.

ACKNOWLEDGEMENT AND REFERENCES

The support of the Ministry of Education, Science and Culture of the Japanese Government(Grant-in-Aid for General Scientific Research) is gratefully acknowledged. The authers would like to express their thanks to Mr. H.Yokogawa, Mr. Y. Ushio and Mr. H.Shimokawa for their cooperation in carrying out the experiments.

(1)Kato B.,"Beam-to-Column Connection Research," Journal of the Structural Division, ASCE, Vol.108, No.ST2, 1982.2

(2)Naka T., Nakao M. and Osano H.,"Restoring Force Characteristics of Steel Beam-to-Column Connections and Aseismicity of Frames," The 27th Symposium on Structural Engineering, 1981.2 (in Japanese)

(3)Nakao M.,"Research on the Behaviour of Steel Beam-to-Column Rigid Connections," Dissertation presented to the University of Tokyo, in 1975, in Partial Fulfillment of the Requirements for the Degree of Doctor of Eingineering (in Japanese)

(4)Kawano A. and Makino M.,"On the Effect of Shear Stiffening of Beam-to-Column Connections in Aseismic Design of Low-rise Steel Frames," Trans. of the A.I.J., (Part I) No.319, 1982.9, (Part II) No.334, 1983.12 (in Japanese)

(5)Fielding D.J. and Huang J.S.,"Shear in Beam-to-Column Connections," The Welding Journal, Vol.50, 1971.7

(6)Krawinkler H. and Popov E.P.,"Seismic Behavior of Moment Connections and Joints," Journal of Structural Division, ASCE, Vol.108, No.ST2, 1982.2

(7)Matsuo A. and Mukudai Y.,"A Study on the Behavior of Strain at the End of the Beam of Steel Multi-Stroied Building Subjected to Severe Earthquakes," Trans. of the A.I.J., No.313, 1982.3 (in Japanese)

(8)Yamada Y.,"Strength of Materials for Matrix Methods of Structural Analyses," Baifukan Press, 1970.11 (in Japanese)

Table 1 Details of specimens

Specimen	Column	Beam	L_b (cm)	L_{ct} (cm)	L_{cb} (cm)	$\frac{b}{t_f}$ *	$\frac{d}{t_w}$ *	Materials ** CF	CW	BF	BW	α	R_{py}
TMB0-3-0850A	H-180X150X4.5X 12	H-180X150X3.2X 9	161.0	40.9	40.9	8.3	50.6	15	10	13	8	0.28	0.39
TMB0-3-0850B	H-180X150X4.5X 12	H-180X150X3.2X 9	161.0	24.2	24.2	8.3	50.6	15	10	13	8	0.28	0.49
TMB0-4-1050	H-160X120X3.2X 6	H-160X120X3.2X 6	130.2	34.5	34.5	10.0	46.3	5	2	6	1	0.35	0.49
TMB0-5-1050A	H-170X120X4.5X 12	H-170X120X3.2X 6	161.0	47.2	47.2	10.0	49.4	15	10	11	9	0.54	0.73
TMB0-5-1050B	H-160X120X4.5X 12	H-160X120X3.2X 6	130.2	30.0	30.0	10.0	46.3	5	2	6	3	0.54	0.79
TMB0-4-1230	H-135X144X4.5X 12	H-135X144X4.5X 6	130.0	38.5	38.5	12.0	27.3	4	3	6	3	0.39	0.54
TMB0-3-1250	H-160X144X3.2X 12	H-160X144X3.2X 6	170.0	29.5	29.5	12.0	46.3	4	1	6	1	0.32	0.49
TMB0-4-1250A	H-170X150X4.5X 12	H-170X150X3.2X 6	161.0	48.2	48.2	12.5	49.4	14	10	12	7	0.40	0.52
TMB0-4-1250B	H-170X150X4.5X 12	H-170X150X3.2X 6	140.0	26.7	26.7	12.5	49.4	15	10	12	7	0.40	0.64
TMB0-5-1250	H-160X144X 6 X 12	H-160X144X3.2X 6	170.4	29.0	29.0	12.0	46.3	4	1	6	4	0.51	0.79
TMC0-5-0820	H-100X 69X4.5X4.5	H-170X 69X 6 X12	151.0	62.1	52.1	7.7	20.2	17	17	20	18	0.50	0.59
TMC0-3-1130A	H-100X 71X3.2X3.2	H-100X 71X 6 X12	130.0	63.3	53.3	10.9	29.3	16	16	19	18	0.27	0.32
TMC0-3-1130B	H-150X103X4.5X4.5	H-170X103X 6 X12	145.0	64.5	54.5	11.4	31.3	17	17	19	18	0.33	0.40
TMC0-5-1125	H-130X 96X4.5X4.5	H-230X 96X 6 X12	151.0	63.8	53.8	10.7	26.9	17	17	20	18	0.50	0.59
XMC0-4-0920	H-110X110X 6 X 6	H-150X110X4.5X 6	150.0	90.0	70.0	9.2	16.3	21	21	22	21	0.34	0.42
XMC3-4-0920A	H-110X110X 6 X 6	H-150X110X4.5X 6	150.0	90.0	70.0	9.2	16.3	21	21	22	21	0.42	0.53
XMC3-4-0920B	H-110X110X 6 X 6	H-150X110X4.5X 6	150.0	80.0	80.0	9.2	16.3	21	21	22	21	0.42	0.53
XMC0-4-1120A	H-100X100X4.5X4.5	H-150X100X4.5X 6	150.0	90.0	70.0	11.1	20.2	22	22	22	21	0.37	0.40
XMC0-4-1120B	H-100X100X4.5X4.5	H-150X100X4.5X 6	150.0	80.0	80.0	11.1	20.2	22	22	22	21	0.37	0.40
XMC3-4-1120A	H-100X100X4.5X4.5	H-150X100X4.5X 6	150.0	90.0	70.0	11.1	20.2	22	22	22	21	0.44	0.56
XMC3-4-1120B	H-100X100X4.5X4.5	H-150X100X4.5X 6	150.0	80.0	80.0	11.1	20.2	22	22	22	21	0.44	0.56
XMC3-4-1130	H-100X100X3.2X4.5	H-240X100X4.5X 6	150.0	70.0	70.0	11.1	28.4	24	23	27	25	0.45	0.56
XMC3-4-1140	H-130X100X3.2X4.5	H-240X100X4.5X 6	150.0	70.0	70.0	11.1	37.8	24	23	26	25	0.43	0.55
XMC3-4-1230	H-100X110X3.2X4.5	H-240X100X4.5X 6	150.0	70.0	70.0	12.2	28.4	24	23	27	25	0.42	0.52
XMC3-4-1240	H-130X110X3.2X4.5	H-240X100X4.5X 6	150.0	70.0	70.0	12.2	37.8	24	23	26	25	0.40	0.50
TMC3-4-1130	H-100X100X3.2X4.5	H-240X100X4.5X 6	150.0	70.0	70.0	11.1	28.4	24	23	27	25	0.45	0.56
TMC3-4-1140	H-130X100X3.2X4.5	H-240X100X4.5X 6	150.0	70.0	70.0	11.1	37.8	24	23	26	25	0.42	0.53
XMC3-2-1130	H-100X100X3.2X4.5	H-140X100X4.5X 6	150.0	70.0	70.0	11.1	28.4	24	23	27	24	0.26	0.34
XMC3-2-1140	H-130X100X3.2X4.5	H-140X100X4.5X 6	150.0	70.0	70.0	11.1	37.8	24	23	26	24	0.24	0.30
XMC3-2-1230	H-100X110X3.2X4.5	H-140X100X4.5X 6	150.0	70.0	70.0	12.2	28.4	24	23	27	24	0.25	0.29
XMC3-2-1240	H-130X110X3.2X4.5	H-140X100X4.5X 6	150.0	70.0	70.0	12.1	37.8	24	23	26	24	0.22	0.28

* b/t_f, d/t_w: width-to-thickness ratio of flanges and webs

** Materials correspond to Group No. in Tab.2
CF: column flange, CW: column web, BF: beam flange, BW: beam web

Table 2 Mechanical properties

Group	σ_y t/cm²	σ_b t/cm²	ε_{st}	E_{st} t/cm²	ε_f
1	2.99	4.25	0.0115	24.0	0.28
2	2.38	3.37	0.0205	19.0	0.27
3	3.23	4.74	0.0145	26.0	0.24
4	2.54	3.46	0.0130	18.0	0.21
5	2.84	3.67	0.0200	17.0	0.21
6	2.71	4.32	0.0170	38.0	0.23
7	2.59	3.71	0.0152	24.5	0.29
8	2.50	3.73	0.0129	28.2	0.27
9	2.56	3.79	0.0149	27.3	0.31
10	2.48	3.53	0.0107	22.4	0.30
11	2.20	3.52	0.0114	32.2	0.31
12	2.51	3.89	0.0125	24.9	0.29
13	2.60	3.73	0.0136	23.7	0.31
14	2.65	4.53	0.0118	48.3	0.27
15	2.63	4.54	0.0098	45.2	0.29
16	2.76	4.28	0.0118	44.6	0.28
17	3.42	4.57	0.0143	84.9	0.24
18	3.32	4.35	0.0203	61.7	0.23
19	2.81	4.35	0.0104	96.8	0.28
20	2.78	4.66	0.0129	88.7	0.25
21	3.37	4.51	0.0287	35.4	0.35
22	3.95	4.71	0.0269	17.0	0.29
23	3.12	3.97	0.0200	19.9	0.28
24	3.77	4.53	0.0264	28.3	0.27
25	2.89	3.92	0.0218	29.6	0.35
26	3.29	4.46	0.0200	28.3	0.30
27	4.28	4.96	0.0255	19.2	0.27

Notes
σ_y: yield stress, σ_b: tensile strength
ε_{st}: strain at the onset of strain hardening
E_{st}: strain hardening modulus
ε_f: elongation

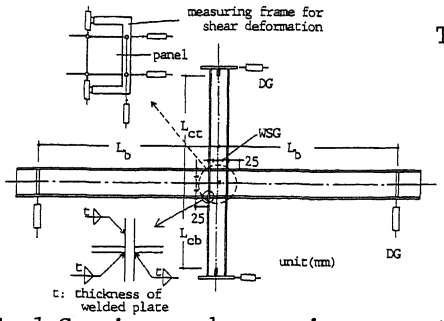

Fig.1 Specimen and measuring apparatus

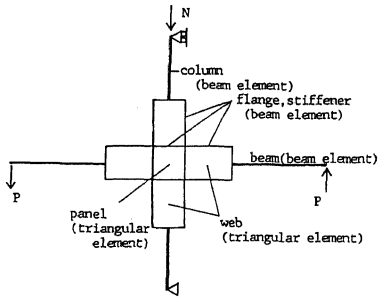

Fig.2 Analytical model of subassemblages

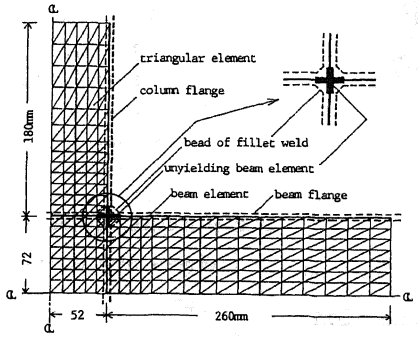

Fig.3 Example of mesh division(XMC0-4-0920)

Table 3 Non-dimensional moment along flanges

specimen	γ/γ_y	flange M/M_{Fu} (M/M_{Fp})	stiffener M/M_{Fu} (M/M_{Fp})
TMB0-3-0850A	14.3 35.8	0.91 (1.43) 1.01	0.70 (1.21) 0.84
TMB0-4-1050	11.4 40.7	0.94 (1.36) 1.01	0.75 (1.28) 0.99
TMB0-3-1250	13.9 22.1	0.85 (1.31) 0.99	0.81 (1.27) 0.89
TMB0-4-1250A	15.5 26.8	1.13 (2.04) 1.22	0.55 (0.93) 0.58
XMC0-4-0920	8.1 26.8	0.74 (1.00) 0.89	0.82 (1.11) 1.02
XMC3-4-0920B	12.9 20.5	0.73 (1.05) 0.79	0.88 (1.06) 0.94
XMC3-2-1130	17.6 31.7	0.81 (0.99) 0.86	0.91 (1.24) 1.02
XMC3-2-1140	11.3 24.5	0.81 (0.99) 0.89	0.86 (1.17) 0.97

Table 4 Predicted maximum panel moment

Specimen	L_r ($\times t_f$) column	beam	p^{MG}_{Ti} (tcm)	p^{MG}_{Ti} (tcm)	$\frac{p^{MG}_{Ti}}{p^{MG}_{Ti}}$
TMB0-3-0850A	1.12	1.38	426	431	0.99
TMB0-4-1050	1.02	1.86	283	296	0.96
TMB0-5-1050B	1.12	1.51	303	311	0.97
TMB0-4-1230	1.09	1.68	315	331	0.95
TMB0-3-1250	1.11	1.59	296	322	0.92
TMB0-4-1250A	1.00	1.28	375	365	1.03
TMB0-5-0820	2.13	1.14	229	227	1.01
TMC0-3-1130A	2.63	1.00	103	124	0.83
TMC0-3-1130B	1.40	1.10	327	339	0.96
TMC0-5-1125	2.17	1.07	383	381	1.01
XMC0-4-0920	1.50	1.44	298	354	0.84
XMC3-4-0920A	1.73	1.60	302	308	0.98
XMC3-4-0920B	1.72	1.58	329	302	1.09
XMC0-4-1120A	2.19	1.55	221	280	0.79
XMC0-4-1120B	2.15	1.59	222	257	0.86
XMC3-4-1120A	2.09	1.61	222	228	0.97
XMC3-4-1120B	2.04	1.51	222	217	1.02
XMC3-4-1140	1.99	1.80	261	240	1.09
XMC3-4-1230	2.25	1.90	223	222	1.00
XMC3-4-1240	2.08	1.54	265	247	1.07
XMC3-4-1130	1.90	1.79	197	186	1.06
XMC3-4-1140	2.04	1.81	243	224	1.08
XMC3-2-1130	2.60	1.94	154	159	0.97
XMC3-2-1140	2.59	1.41	173	180	0.96
XMC3-2-1230	2.09	1.72	150	169	0.89

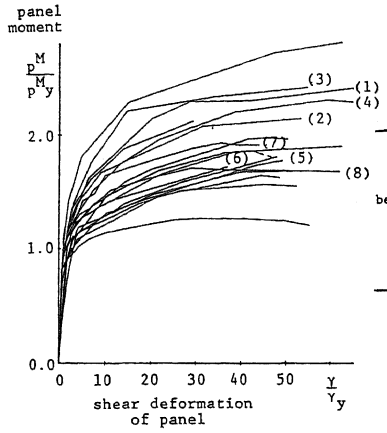

Fig.4 Experimental results

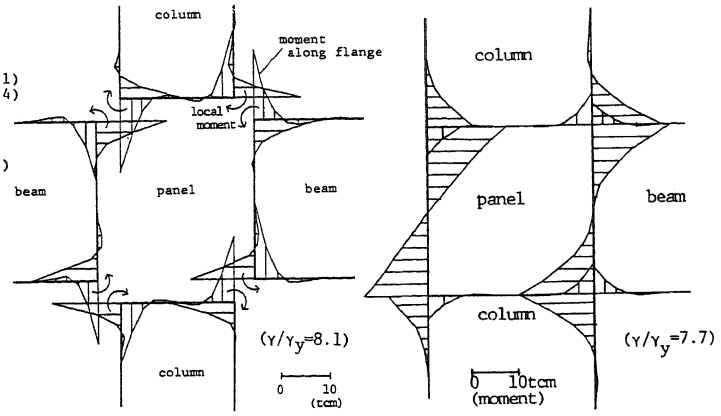

(a)XMC0-4-0920 (b)TMB0-4-1050

Fig.6 Moment distribution along flanges

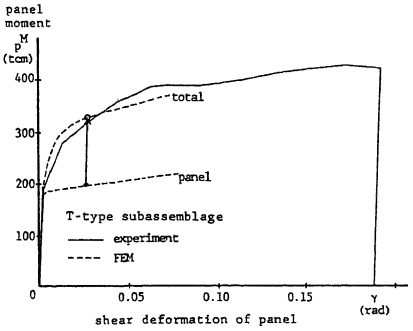

(a)TMB0-3-0850A

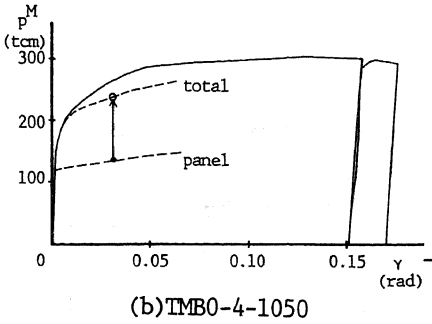

(b)TMB0-4-1050

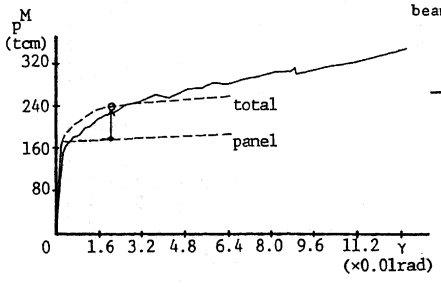

(c)XMC0-4-0920

Fig.5 Analytical results

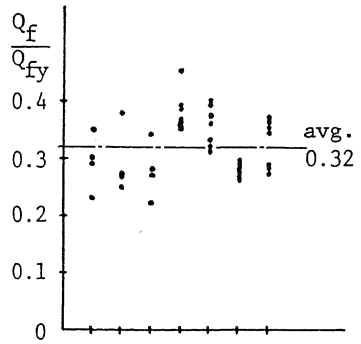

Fig.8 Shear force at unyielding elements

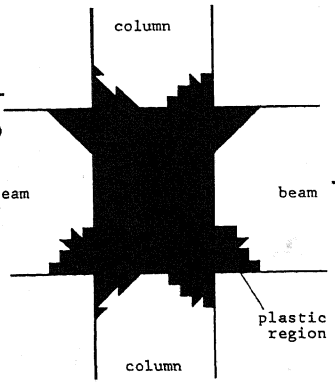

Fig.7 Plastic regions around connection

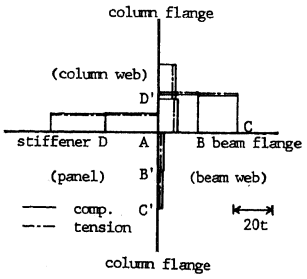

Fig.9 Axial force along flanges and stiffners